7108–7123 Nucleic Acids Research, 2018, Vol. 46, No. 14 Published online 9 June 2018
doi: 10.1093/nar/gky484

Regulation of miR-34b/c-targeted gene expression program by SUMOylation

Yi-Jia Li[1], Li Du[1], Grace Aldana-Masangkay[1], Xiuli Wang[2], Ryan Urak[2], Stephen J. Forman[2], Steven T. Rosen[2] and Yuan Chen[1,*]

[1]Department of Molecular Medicine, Beckman Research Institute of the City of Hope, Duarte, CA 91010, USA and [2]Department of Hematology and Hematopoietic Cell Transplantation, Beckman Research Institute of the City of Hope, Duarte, CA 91010, USA

Received September 26, 2017; Revised May 14, 2018; Editorial Decision May 15, 2018; Accepted May 22, 2018

ABSTRACT

The miR-34 family of microRNAs suppresses the expression of proteins involved in pluripotency and oncogenesis. miR-34 expression is frequently reduced in cancers; however, the regulation of their expression is not well understood. We used genome-wide miRNA profiling and mechanistic analysis to show that SUMOylation regulates miR-34b/c expression, which impacts the expression of c-Myc and other tested miR-34 targets. We used site-directed mutagenesis and other methods to show that protein kinase B (also known as Akt) phosphorylation of FOXO3a plays an important role in SUMOylation-dependent expression of miR-34b/c. This study reveals how the miR-34-targeted gene expression program is regulated by SUMOylation and shows that SUMOylation need not regulate target proteins through direct modification, but instead can act through the expression of their targeting miRNAs.

INTRODUCTION

microRNAs (miRNAs/miRs) regulate gene expression by pairing with messenger RNA (mRNA) to inhibit translation and induce degradation. miRNAs are first transcribed as pri-miRNAs, which are processed to yield pre-miRNAs, then further processed to become mature miRNAs (1). The miR-34 family of miRNAs is composed of tumor suppressors that target the major human oncogene MYC and other important genes involved in oncogenesis, such as BCL-2, the E2F family, CDK4, Yin Yang 1 (YY1) and MET (2–7). The miR-34 family is often down-regulated in tumors; conversely, increasing miR-34 levels results in suppression of cancer cell proliferation and induction of apoptosis (8–13). However, the pathways regulating miR-34 expression are not yet fully understood.

Small ubiquitin-like modifiers (SUMO) are ubiquitin homologues that covalently link to other cellular proteins through a biochemical mechanism similar to ubiquitination (14,15). SUMOylation requires several enzymes that catalyze three steps: activation by the E1 (heterodimer of SAE1 and SAE2, also known as Uba2), conjugation by E2 (also known as Ubc9), and ligation by one of approximately ten E3 ligases. SUMO modification adds a new docking site to target proteins. This enables new protein-protein interactions through the SUMO-interacting motif (SIM) in receptor proteins (16,17). The role of SUMOylation in the transcription of non-coding RNAs, including pri-miRNAs, is not well understood.

In this study, we used genome-wide miRNA-seq and mRNA-seq profiling and biochemical and molecular biological investigation to reveal that SUMOylation plays an important role in the transcription of the pri-miRNA of miR-34b/c, but not miR-34a. miR-34a, b and c share the same seed sequence and thus are thought to target the same mRNAs. The coding DNA sequences of miR-34b and c are adjacent to each other and are believed to be processed from the same primary transcript (18), but the coding DNA sequence of miR-34a is located on a different chromosome from that of miR-34b/c. We showed that knockdown of SAE2 or Ubc9 led to increased levels of mature miR-34b/c, but not miR-34a, and down-regulated the mRNA and proteins of their targets, including c-Myc. We observed these effects in multiple cell lines representing solid tumors and hematological malignancies. We found that SUMOylation regulates the expression of miR-34b/c through Akt phosphorylation of FOXO3a, suggesting a mechanism for miR-34b/c down-regulation in cancer cells. Because it was shown previously that c-Myc activates SUMOylation (19), this study reveals a feed-forward mechanism between c-Myc and SUMOylation. Furthermore, our results indicate that a post-translational modification need not regulate a target protein through direct modification, but instead can act through altering the expression of miRNAs that target the protein.

*To whom correspondence should be addressed. Tel: +1 626 215 4152; Email: ychen@coh.org

© Crown copyright 2018.
This article contains public sector information licensed under the Open Government Licence v3.0 (http://www.nationalarchives.gov.uk/doc/open-government-licence/version/3/).

MATERIALS AND METHODS

Cell culture and lentivirus production

Colon cancer cell lines were grown in DMEM. Lymphoma cell lines and multiple myeloma RPMI-8226 cell line were maintained in RPMI-1640. Media were supplemented with 10% heat inactivated fetal calf serum (Omega Scientific, Inc.), 2 mM L-glutamine, 100 U ml^{-1} penicillin, and 100 $\mu g\ ml^{-1}$ streptomycin. HCT116 and RPMI-8226 cells were stably transfected with tetracycline (Tet) suppressor (TR) expression plasmid pcDNA6/TR before transduction with lentivirus containing Tet-On short hairpin RNA (shRNA) targeting the SAE2 mRNA (Tet-On shSAE2). Stably transfected cells were selected using 5 μg/ml blasticidin. HCT116 and RPMI-8226 cells stably expressing TR were used for lentivirus transduction within one to two passages after blasticidin selection. For lentivirus generation, the envelope plasmid pCMV-VSVG and the packaging plasmid pCMV-dR8.2-dvpr were obtained from Addgene (8454 and 8455, provided by Dr Bob Weinberg). Inducible SAE2 shRNAs were purchased from GE Dharmacon (V2THS_254939 and V2THS_68114). Inducible human Myc shRNA was also purchased from GE Dharmacon (V2THS_152051). 293T producer cells were transfected with these vectors, and supernatant containing lentiviral particles was harvested 24–48 h after transfection. Then the cells were transduced with two different Tet-On shSAE2 lentiviruses and the stably transduced cells were selected with puromycin (5 μg/ml) 2 days after viral transduction. For doxycycline (DOX)-induced SAE2 knockdown, 2–5 μg/ml DOX was added to cells for 3–5 days to induce knockdown. A stable Tet-On SAE2-GFP-expressing HCT116 cell line was established using lentiviral transduction. Briefly, the cells were transduced with Tet-On SAE2-GFP lentivirus and stably transformed cells were selected with puromycin (5 μg/ml) 2 days after viral transduction.

Soft agar colony formation assay

For SAE2 knockdown, HCT116 cells were suspended in 1 ml of 10% FBS DMEM medium containing 0.3% agarose with or without DOX at 5 μg/ml and plated in triplicate on a firm 0.6% agarose base in 12-well plates (1000 cells/well). Cells were placed in a 37°C, 5% CO_2 incubator. Colonies of cells were allowed to grow over the course of 2 weeks. Images were obtained using a camera (Optronics) mounted to a microscope. Colonies with a diameter greater than 50 μm were counted under a microscope (Nikon ECLIPSE TE300). The colony formation assay was performed in triplicate.

For pre-miRNA transfection, HCT116 cells were counted and plated in 24-well soft agar plates 5 days after transfection, then continually cultured for 21 days before the tumor spheroids were counted.

Cell viability assay

Cell viability was measured using a CellTiter-Glo viability assay kit (Promega) after SAE2 knockdown or pre-miRNA or short interfering RNA (siRNA) transfection. Briefly, cells were allowed to equilibrate to room temperature, at which time 100 μl of Cell Titer-Glo reagent mixture was added. Cells were placed on a rocking shaker for 5 min and incubated for an additional 5 min on the bench top. Luminescent measurements were performed using a CLARIOstar (BMG LabTech) reader. For assays measuring anti-proliferation effects, all values were normalized to the no-DOX treatment or control siRNA/pre-miRNA transfections. All values are represented graphically as mean ± standard deviation (STDEV) from three independent samples.

Flow cytometry-based apoptosis assay

DOX-treated, siRNA- or pre-miRNA-transfected, or shSAE2-GFP lentivirus-transduced cells were harvested with trypsin-EDTA, then resuspended in PBS containing 1% (m/v) bovine serum albumin (BSA) (10^6 cells/ml for each experimental condition). Detection of apoptosis in tumor cells in suspension was performed using the Annexin V apoptosis detection kit (Life Technology). The staining was analyzed on a CyAn ADP flow cytometry instrument (Beckman Coulter, Inc.). Analysis of the data was performed using software Summit 4.3 (Beckman Coulter, Inc.).

Immunoprecipitation and Western blot

In general, cells were harvested 48 h after DNA transfection or 120 h after siRNA transfection or DOX-induced SAE2 knockdown. After washing twice with 1× PBS, the cells were directly lysed in 2× SDS sample buffer (4% SDS, 20% glycerol, 0.004% bromophenol blue, and 0.125 M Tris–HCl pH ~6.8). Samples were sonicated for 3 × 10 s to shear DNA and quantitated using BCA protein assay kit. 2 M β-mercaptoethanol was added to the protein samples, which were then boiled at 95°C for 5 min, before separation using SDS-PAGE, and Western blotting. Western blot results were visualized using the Odyssey IR imager (LI-COR) that can detect both IRDye 680- and 800-conjugated secondary antibodies (1:10 000). Quantification of Western blots was performed using Odyssey IR software, version 1.2 (LI-COR). For Akt immunoprecipitation and Western blot, anti-Akt antibody (40D4, mouse mAb; Cell Signaling) was first used for immunoprecipitation. Anti-SUMO1 (C9H1; rabbit mAb; Cell Signaling) and Clean-Blot IP Detection Kit (Thermo Scientific) were used for Western blot.

Antibodies for western blot, chromatin immunoprecipitation (ChIP), immunohistochemistry (IHC) and immunofluorescence (IF)

The following rabbit antibodies used for Western blot, ChIP, IHC or IF were all from Cell Signaling Technology (1:1000): anti-SUMO1 (C9H1) mAb, anti-c-Myc (D84C1) mAb, anti-c-Met (D1C2) XP mAb, anti-Jun (60A8), anti-Bcl2 (#2872), anti-YY1 (13G10), anti-SP1 (D4C3), anti-HA-tag (C29F4), anti-FOXO3a (D19A7), and anti-p-FOXO3a (Ser253). Anti-CTCF, anti-Myb, anti-E2F3 (N2C3) and anti-CDK4 (GTX102993) were from GeneTex. Anti-E2F1 (KH95) and anti-GAPDH (I19) were from Santa Cruz Biotechnology. Rabbit anti-SAE2/UBA2 (1:1000) (ab58451), mouse anti-SAE2 (ab118404) and anti-SAE1 (ab185949) were from Abcam. Mouse monoclonal

antibody against SUMO2/3 (1E7) was from MBL Medical & Biological Laboratories Co., Ltd. Rabbit anti-c-Myc (ab32072) from abcam was used for IHC to validate c-Myc expression in mouse xenograft tumor.

ChIP experiments

After 5 days of DOX-induced SAE2 knockdown, the cells were fixed in 1% formaldehyde at room temperature for 15 min. After quenching the formaldehyde by adding 2 M glycine to a final concentration of 125 mM, the cells were harvested and resuspended in lysis buffer (1% SDS, 10 mM EDTA pH 8, 50 mM Tris–HCl pH 8, 0.2% NP-40, 10 mM NaCl) containing 20 mM *N*-ethylmaleimide (NEM) and protease inhibitor cocktail (Roche). Following sonication at 25% power for 10 × 15 s, the cell extract was then diluted and incubated with antibody against various transcription factors or 2 μg/ml rabbit/mouse IgG at 4°C for 16 h. Protein G Dynabeads were blocked with 5% BSA and salmon sperm DNA at 10 μg/ml for 1 h at room temperature, then added to the samples, which were rotated for 60 min at 4°C. The beads were then washed four times in 1× RIPA buffer (25 mM Tris pH 7–8, 150 mM NaCl, 0.1% SDS, 0.5% sodium deoxycholate, 1% Triton X-100 or NP-40]. After the last wash, the DNA was eluted in elution buffer (50 mM $NaHCO_3$, 1% SDS) and incubated in a 65°C water bath for 15 min. 5 μl of Proteinase K (50 mg/ml, Roche, PCR-grade) was added to the DNA elution, incubated at 42°C for 2 h, and subsequently incubated at 65°C for 16 h to reverse the cross-linking. Qiagen DNA purification kit was then used for further DNA purification. Immunoprecipitated DNA was analyzed using SYBR Green real-time qPCR (SYBR Select Master Mix; Life Technology) according to manufacturer's protocol. Real-time PCR was performed using an Applied Biosystems 7900HT real-time PCR system. The data were analyzed relative to control (without DOX treatment, DOX-) to include normalization for both background levels and the amount of input DNA used in ChIP.

Primers for site-directed mutagenesis, ChIP analysis, and qRT-PCR

For ChIP assay: miR-34b/c promoter forward (F), 5′-CGGCTCCCGGCCTGGGA and reverse (R), 5′-ACACCCCCGGGCCCAGC. For miR-34b/c binding site mutation in pMirTarget-Met-3′UTR: miR34-d2-F, 5′-GGGAGTAAGTGATTCTTCTAAGAATTA GATACTTGTTATACCTGCAGCTGAACTGAA TGGTACTTCG-3′ and miR34-d2-R, 5′-CGAAGTA CCATTCAGTTCAGCTGCAGGTATAACAAGT ATCTAATTCTTAGAAGAATCACTTACTCCC.
For miR-34b/c promoter subcloning to luciferase reporter plasmid pGL3 (Promega): miR-34b/c-P-F, 5′-ACTGCTCTCGAGTAGCTCCTTTTCCATCTCC-3′ and miR-34b/c-P-R, 5′-GACGATAAGCTTCCGCG CCCTCCCAGGCCGG-3′. For miR-34b/c binding site mutation in pRL c-Myc 3′UTR: MYC-3UTR-mut-F, 5′-CATAATTTTAACTGAAGGGAACTTA AATAGTATAAAAG-3′ and MYC-3UTR-mut-R, 5′-CTTTTATACTATTTAAGTTCCCTTCAGTT AAAATTATG-3′. For Akt K276R/E278A SUMO-deficient mutant: F, 5′-CCTTGTCCAGCATGAGG TTCGCCAGCCTGAGGTCCCGGTACACC-3′ and R, 5′-GGTGTACCGGGACCTCAGGCTGGCGAA CCTCATGCTGGACAAGG-3′. For FOXO3a constitutive phosphorylation mutant TD: FOXO3-T32D-F, 5′-CCGTCCGCGATCCTGTGACTGGCCCCT GCAAAGG-3′ and FOXO3-T32D-R, 5′-CCTTTGC AGGGGCCAGTCACAGGATCGCGGACGG-3′; FOXO3-S253D-F, 5′-CCGGCGGCGGGCTGTCGAC ATGGACAATAGCAACAAGTAT-3′ and FOXO3-S253D-R, 5′-ATACTTGTTGCTATTGTCCATGT CGACAGCCCGCCGCCGG-3′; FOXO3-S315D-F, 5′-GGACTTCCGTTCACGCACCAATGATAACG CCAGCACAGTCAGTGG-3′ and FOXO3-S315D-R, C5′-CACTGACTGTGCTGGCGTTATCATTGG TGCGTGAACGGAAGTCC-3′; and FOXO3-seq, 5′-CCTGTCACTGCATAGTCGATTC-3′. For miR-34b/c target gene expression qRT-PCR: BCL2-F1, 5′-ATGTGTGTGGAGAGCGTCAACC-3′ and BCL2-R1, 5′-TGAGCAGAGTCTTCAGAGACAGCC-3′; CDK4-F, 5′-GTCGGCTTCAGAGTTTCCAC-3′ and CDK4-R, 5′-TGCAGTCCACATATGCAACA-3′; YY1-F, 5′-CAACCACTGTCTCATGGTCAA-3′ and YY1-R, 5′-CAAGAAGTGGGAGCAGAAGC-3′; E2F3-F1, 5′-CTAGCTCCAGCCTTCGCTTT-3′ and E2F3-R1, 5′-AGCCTCCTCTACACCACGC-3′; GAPD-qPCR-F, 5′-AATGAAGGGGTCATTGATGG-3′ and GAPD-qPCR-R, 5′-AAGGTGAAGGTCGGAGTCAA-3′.

RNA extraction, reverse transcription and quantitative real-time PCR (qRT-PCR)

Total mRNA and miRNA were extracted from cells with DOX treatment or DNA transfection using miRNeasy RNA isolation kit (Qiagen) per the manufacturer's protocol. miRNA cDNA was synthesized from total RNA using TaqMan miRNA Reverse Transcription Kit and 5X miRNA specific RT primer (Life Technology) according to manufacturer's protocol. Briefly, reverse transcriptase reactions contained 100 ng of RNA for miR-34b/c samples or 10 ng of RNA for RNU6B samples, 50 nM RT primer, 1× RT buffer, 0.25 mM each of dNTPs, 3.33 U/μl MultiScribe reverse transcriptase and 0.25 U/μl RNase inhibitor. The 15 μl reactions were incubated in an iCycler (Bio-rad) for 30 min at 16°C, 30 min at 42°C, 5 min at 85°C, then held at 4°C. Total RNAs were converted to cDNA using Superscript III reverse transcriptase (Life Technology) and oligo d(T) primer according to manufacturer's protocol. Real-time PCR was performed using an Applied Biosystems 7900HT real-time PCR system. For miRNA cDNA real-time PCR, the 20 μl PCR volume included 1.33 μl RT product, 1× TaqMan Universal PCR master mix (no UNG) (Life Technology) and 1 μl of Taqman Small RNA Assay mix (Life Technology). Taqman Small RNA Assay sets hsa-miR-34c-5p (000428), hsa-miR-34b-5p (000427) and RNU6B (001093) were from Thermo Fisher Life Technology. For real-time PCR of gene expression, the 20 μl PCR volume included 1 μl RT product, 1× TaqMan Gene Expression Master Mix (Life Technology), and 1 μl of TaqMan Gene Expression Assay primer mix (Life Tech-

nology) for pri-miR-34b/c, MYC, MET, and GAPDH (pri-miR-34b/c, Hs03295169_pri; MYC, Hs00153408_m1; MET, Hs01565576_m1; GAPDH, Hs01565576_m1). To measure *E2F3*, *YY1*, *CDK4* and *BCL2* expression levels, power SYBR Green PCR mix (Life Technology) was used according to the manufacture's protocol. The primers for the qPCR are listed above. The reactions were incubated in a 386-well optical plate at 95°C for 10 min, followed by 40–45 cycles of 95°C for 15 s and 60° for 10 min. All quantitative PCR reactions were performed using the 7900HT Fast Real-Time PCR System (Applied Biosystems). The change in threshold cycle (ΔCt) was determined using default threshold settings. Ct is defined as the fractional cycle number at which fluorescence passes the fixed threshold. The relative fold change in expression was measured using the ΔΔ(CT) method between each SAE2 knockdown and the average of the control samples: Δ(CT) = CT(miRNA or miR34 target gene) − CT(RNU6B or GAPDH); ΔΔ(CT) = ΔCT (knockdown) − ΔCT (control); fold change = $2^{-\Delta\Delta(CT)}$.

Statistical analysis

All experiments were carried out at least three independent times. Data shown in bar graphs are mean ± STDEV. *P*-values were evaluated using the analysis of variance (one-way ANOVA) or Student's *t*-test as indicated in the figures and legends. A *P*-value <0.05 was considered statistically significant.

DNA constructs and siRNAs

pcDNA3Myr HA-Akt1 was from Dr William Sellers (Addgene plasmid #9008). pCMV-GFP was from Dr. Connie Cepko (Addgene plasmid #11153). HA-FOXO3a wild type (WT) (Addgene Plasmid #1787), HA-FOXO3a WT DBM (H212R) (Addgene Plasmid #8352) and HA-FOXO3a TM (Addgene Plasmid #1788) were gifts from Dr Michael Greenberg. pCMV-Ubc9 (RC217884) was obtained from Origene. The SAE2-GFP gene was PCR-amplified from pCMV-SAE2-GFP and inserted into pLenti CMV/TO Puro DEST (670-1) to obtain a Tet-On-inducible SAE2-GFP expression plasmid. siRNAs against SAE2, UBC9 and Dicer were obtained from GE Dharmacon SMARTpool.

DNA transient transfection and siRNA transfection

Transient transfection of plasmid DNA was performed using Lipofectamine (LTX; Life Technology) following the manufacturer's instructions. siRNA transfection was performed using Lipofectamine RNAiMAX (Life Technology) according to the manufacturer's instructions. Cells were harvested 48 h after plasmid DNA transfection and lysed directly in buffer containing 190 mM Tris pH 6.8, 30% glycerin and 4% SDS. In addition, cells were re-transfected with siRNA 72 h after the first transfection to ensure siRNA knockdown effects. The cells were then harvested 48 h after the second siRNA transfection and either directly lysed in SDS buffer or used to isolate RNA using the microRNeasy kit (Qiagen) according to manufacturer's instruction.

Ribo-Zero RNA-seq, small RNA-seq, GSEA and cumulative distribution plot

Two HCT116 cell lines with DOX-induced expression of two different shRNA targeting SAE2 (Sh1 and Sh2) were used to perform Ribo-Zero RNA-seq and small RNA-seq. The HCT116 cells were treated with DOX to induce SAE2 knockdown for 5 days before cell harvesting. Total RNA was then purified using a miRNeasy RNA isolation kit (Qiagen) per the manufacturer's protocol. Gene expression profiles of duplicated RNA samples from two independent shRNA against SAE2 were analyzed using Ribo-Zero RNA-seq and small RNA-seq. RNA-seq data processing and analysis were performed by the City of Hope Functional Genomics Core Facility. Briefly, the SMARTer Stranded Total RNA-seq V2-pico Input kit (Takara) was used for sequencing library preparation and single-read 51-bp sequencing was performed using a Hiseq2500 (Illumina). Output files in fastq format were processed for pre-alignment quality control. Further redundant sequences including ribosomal RNAs, transfer RNAs, adapter sequences, and others were filtered using Bowtie or Tophat tool. Pre-processed reads were aligned to human genome (hg19) and the Partek Genomics Suite or Customized R scripts were used for differential gene expression analysis. Normalization was performed using the trimmed mean of *M* values (TMM) method (20) for mRNA-seq data and counts per million (CPM) method for miRNA-seq data.

For Ribo-Zero RNA-seq, significantly differentially expressed gene data was generated using the following parameters: a fold-change cutoff of 1.5 and a false discovery rate (FDR)-adjusted *P*-value < 0.05. For miRNA-seq, significantly differentially expressed miRNAs were evaluated using the following parameters: a fold-change cutoff of 2 and FDR-adjusted *P*-value < 0.05. The low sequence reads filter (cutoff) was set to 20 in control and SAE2-knockdown samples. All RNA-seq and miRNA-seq experiments were performed with two individual DOX-induced shRNA targeting SAE2 at different regions and the ratio of DOX+/DOX- was used to calculate the fold change of gene/miRNA expression.

To confirm the reliability and the comparability of differential expression analysis, gene transcripts with FPKM (Fragments Per Kilobase of transcript per Million mapped reads) ≥ 1 in all samples were examined. A difference in gene expression of 2-fold or more was considered a significant change and included for further analysis. Student's *t*-test was performed for each of the differentially expressed transcripts across the replicate samples.

To perform gene set enrichment analysis (GSEA), gene sets were downloaded from the Broad Institute's MSigDB website (21) (www.broad.mit.edu/gsea/) and data analysis was performed using web-based software. Gene set permutations were used to determine statistical enrichment of the gene sets using the signal-to-noise ratio of DOX– versus DOX+. Expression of miR-34b/c-targeted genes from the dataset (TOYOTA_TARGETS_OF_MIR34B_AND_MIR34C, $N = 395$) and non-targeted genes ($N = 10390$) from RNA-seq were plotted using the cumulative distribution function of Microsoft Excel as previous studies described (22).

Xenograft colorectal cancer models

All experiments with mice were approved by Beckman Research Institute Animal Care and Use Committee and complied with all relevant federal guidelines and institutional policies. HCT116 cells expressing a DOX-inducible shSAE2 were injected subcutaneously into 6- to 8-week-old male Nu/J mice (3.0×10^6 cells per mouse). After 5 days, mice were fed either 5% sucrose water (DOX– group) or 5% sucrose water with 2 mg/ml DOX (DOX+ group). Tumor volume was measured with calipers until the endpoint was reached for the control group. Mice were euthanized using CO_2 inhalation and tumors were excised.

Immunohistochemistry (IHC) and immunocytochemistry (IF)

For IHC staining of c-Myc and c-Met, tumor tissues were fixed in 4% paraformaldehyde, washed with PBS, transferred to 70% ethanol, embedded in paraffin, and IHC was performed according to standard procedures.

For FOXO3a IF, cells were cultured at a low density on 8-well chamber slides (Nunc Lab-Tec II Chamber Slide System, Thermo Scientific) and fixed in 4% paraformaldehyde for 20 min at room temperature. The medium was removed by aspiration, and cells were washed twice with 1X PBS. After cell permeabilization in ice-cold acetone/methanol (1:1) solution, proteins were blocked with 5% normal BSA in 1× PBS for 1 h and incubated with rabbit anti-FOXO3a (1:100 dilution; Cell Signaling) for 16 h. After three washes with 1X PBS with 1% BSA, cells were then incubated with Alexa488-conjugated anti-rabbit IgG (Invitrogen) for 1 h at room temperature and counterstained with DAPI. After three washes with PBS, cells were mounted in ProLong Gold Anti-fade Mounting (Life Technology). Immunofluorescence was detected under a fluorescence microscope.

Cell fractionation

5×10^6 cells with/without SAE2 knockdown were harvested, washed twice with cold PBS, and placed into a pre-chilled microcentrifuge tube. Cells were resuspended in 500 μl 1× hypotonic buffer (20 mM Tris–HCl pH 7.4, 10 mM NaCl, 3 mM $MgCl_2$) by pipetting up and down several times and incubated on ice for 15 min. 25 μl detergent (10% NP40) was added to the tube and the mixture was vortexed for 10 s. The homogenate was then centrifuged for 10 min at 800 g at 4°C. The supernatant was transferred and saved as the cytoplasmic fraction. The pellet (nuclear fraction) was resuspended in 50 μl 1× RIPA buffer for 30 min on ice and sonicated for 3 min (30 s on and 30 s off).

SUMO-modified protein purification

FOXO3a was expressed in HeLa, HeLa-His_6-SUMO1 and HeLa-His_6-SUMO2 cell lines by DNA transfection for 2 days, and SUMO-modified FOXO3a was examined as described previously (23). Briefly, cells were directly lysed in cell lysis buffer (6 M guanidinium–HCl, 10 mM Tris, 100 mM sodium phosphate buffer pH 8.0, and 2 mM DTT) after harvesting, then imidazole was added to 5 mM, followed by sonication for 30 s at medium power with a small probe. After centrifugation at 3000*g* for 15 min to remove cell debris, the supernatant was incubated with pre-washed Ni^{2+} NTA beads at 4°C overnight. The beads were spun down for 2 min at 750*g* at room temperature and the supernatant was discarded. Washes were carried out by resuspending the beads in two different buffers, followed by centrifugation for 2 min at 750*g* at room temperature and removal of the supernatant. The first wash buffer contained 1 ml of cell lysis buffer with 5 mM β-mercaptoethanol (8 M Urea, 10 mM Tris, 100 mM sodium phosphate buffer pH 8.0, 0.1% (vol/vol) Triton X-100 and 5 mM β-mercaptoethanol), and three washes were carried out. The second wash buffer (pH 6.3) contained 8 M Urea, 10 mM Tris, 100 mM sodium phosphate buffer pH 6.3, 0.1% (vol/vol) Triton X-100, and 5 mM β-mercaptoethanol, and three washes were carried out. All steps were processed using an aspirator fitted with a flat-ended pipette tip. Proteins were eluted by adding 50 μl of elution buffer (200 mM Imidazole, 5% (w/v) SDS, 150 mM Tris–HCl pH 6.7, 30% (vol/vol) glycerol, 720 mM β-mercaptoethanol, and 0.0025% (wt/vol) bromophenol blue) to each sample, flicking to mix and incubating for 20 min at room temperature to elute the proteins.

RESULTS

SAE2 knockdown increases miR-34b/c but not miR-34a expression

We first established cell lines that can be induced to express shRNA targeting the catalytic subunit of the SUMO E1 enzyme, SAE2. To rule out non-specific shRNA effects, we established separate cell lines using two independent shRNAs, in both colon cancer (HCT116) and multiple myeloma (RPMI-8226) cell lines. We also used siRNA to silence SAE2 gene expression in an Epstein-Barr virus (EBV)-transformed lymphoblastoid cell line (LCL), a model of B-cell malignancy. SAE2 knockdown and suppression of SUMOylation were confirmed (Supplementary Figure S1). SAE2 has a long lifespan, with a half-life of more than twenty-four hours (24); therefore, knockdown of SAE2 protein levels by more than 70% required induction of shRNA expression for three days or longer.

The role of SUMOylation in regulating miRNA expression is poorly understood; therefore, we performed genome-wide miRNA profiling (miRNA-seq) of cells in the absence and presence of SAE2 knockdown. We compared samples prepared using two independent shRNAs, to identify miRNAs that reproducibly increased or decreased by more than 2-fold (Supplementary Table S1). We found that miR-549, miR-181a/b and miR-34c were up-regulated more than 3-fold and that miR-548 was down-regulated more than 3-fold by SAE2 knockdown (Figure 1A). Although miR-34b level also increased upon SAE2 knockdown (Supplementary Figure S2A, right panel; Supplementary Figure S2B, left panel), its expression level as determined by miRNA-seq was low, and it was filtered out along with other low-expression miRNAs using a cut-off of 20 count, and thus did not appear in Figure 1A. In contrast to the increased levels of miR-34b/c, the level of miR-34a did not show a significant increase upon SAE2 knockdown (Supplementary Figure S2A, left panel; Supplementary Figure S2B, left panel).

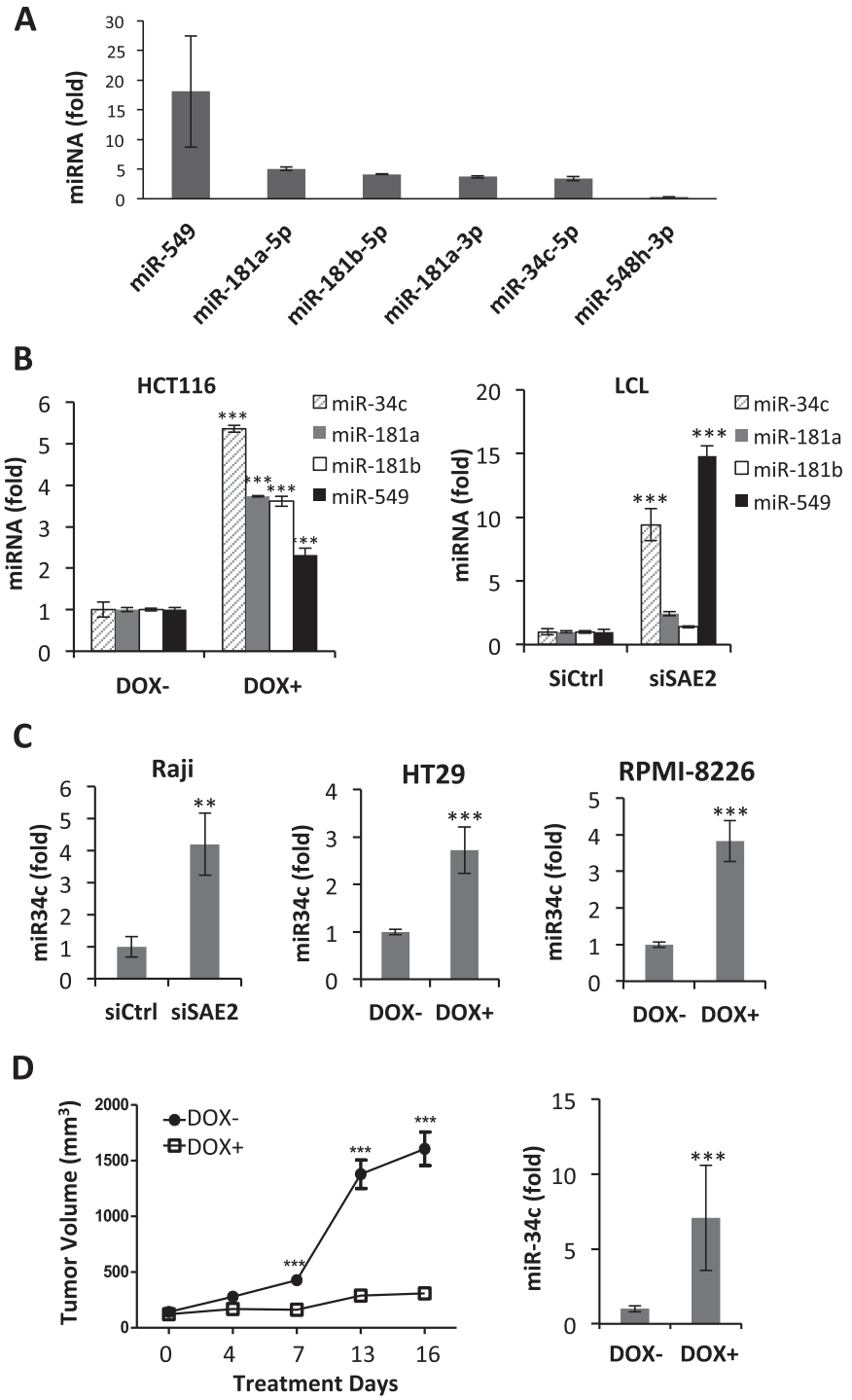

Figure 1. miRNA profiling upon SUMOylation inhibition. (**A**) Six miRNAs that are most affected by SUMOylation inhibition (increased or decreased >3-fold). miRNA profiling was analyzed from two individual SAE2 shRNA (Sh1 and Sh2) knockdown for 5 days in HCT116 cells. Significant changes of miRNAs were evaluated using the following parameters: a fold-change cutoff of 2 and a false discovery rate (FDR)-adjusted *P*-value less than 0.05. Low sequence reads filter (cutoff) was set to 20. Results shown as the mean with difference (error bar) of the miRNA change from two independent shRNA knockdown. (**B**) Examination of the most increased miRNAs using qRT-PCR in HCT116 (left) and LCL (right) cells. DOX was added to induce SAE2 knockdown (DOX+) in HCT116 cells. siRNA against SAE2 (siSAE2) or non-targeting control siRNA (SiCtrl) was used in LCL cells. (**C**) miR-34c levels in the lymphoma cell line Raji, colorectal cancer line HT29, or multiple myeloma cell line RPMI-8226 after SAE2 knockdown. (**D**) HCT116 cells transduced with DOX-inducible SAE2-targeting shRNA were transplanted into nude mice by subcutaneous injection. Recipient mice were treated with (DOX+) or without (DOX–) DOX. Knockdown of SAE2 expression suppressed colorectal tumor growth (left), and increased miR-34c levels in xenograft tumor tissues (right). In all qRT-PCR experiments, miRNA level was first normalized to RNU6B measured from the same RNA sample. miRNA level in the knockdown group was then normalized to that without knockdown. Results shown as mean ± STDEV from three independent experiments. Statistical significance between two groups of animal data in (D) were analyzed by Student's *t* test. For statistical analysis of all qRT-PCRs, one-way ANOVA was used to calculate *P*-value. $^{**}P < 0.01$; $^{***}P < 0.001$.

We then verified miRNA-seq results using qRT-PCR (Figure 1B). To determine whether up-regulation of these miRNAs occurs in different cell lines, we examined the effects of SAE2 knockdown in both HCT116 (shRNA) and LCL (siRNA). Although SAE2 was knocked down in both cell lines (Supplementary Figure S1), miR-181a and -181b levels were elevated in HCT116 cells only, whereas miR-34c and miR-549 were elevated in both cell lines (Figure 1B). miR-34b/c increase were induced by knocking down of SAE2 in a range of cancer cell lines, including Raji, HT29, and RPMI-8226 (SAE2 knockdown in HT29 was described previously (25)) (Figure 1C). We knocked down SAE2 in mouse xenografts of HCT116 cells expressing DOX-inducible SAE2-targeting shRNA; tumor volume following SAE2 knockdown was significantly reduced and miR-34b/c levels were significantly increased compared to control (Figure 1D).

Next, we investigated the effects of increased miR-34b/c and miR-549 expression. We transfected pre-miRNAs of miR-34c and -549 into HCT116 and LCL cells. Transfection of pre-miR-34c into either cell line resulted in significantly reduced cell viability and increased apoptosis relative to control transfection, whereas viability and apoptosis following transfection of pre-miR-549 were not significantly different from control (Figure 2A, B, D and E). We also measured tumor formation ability in a 3D soft agar-based assay after pre-miRNA transfection of HCT116 and LCL cells. Cells transfected with control or pre-miRNA-549 formed spheroids, representative of tumorigenic growth, but pre-miR-34c-transfected cells did not (Figure 2C and F). Taken together, miR-34c elevation upon SAE2 knockdown showed strong anti-tumor effects in both HCT116 and LCL, but miR-549 elevation did not. Knockdown of key SUMOylation enzymes (SAE2, Ubc9) or overexpression of dominant-negative Ubc9 inhibits proliferation, and induces apoptosis, senescence, and G2/M cell cycle arrest in various tumor types (26–29). Based on our findings, we suggest that increased miR-34b/c and not miR-549 expression likely contribute to these anti-tumor effects.

SUMOylation regulates miR-34 target genes in a miRNA-dependent manner

We performed genome-wide mRNA-seq on the same samples used for miRNA-seq. Consistent with increased miR-34b/c expression, GSEA of mRNA-seq data showed that miR-34b/c target genes were significantly down-regulated after SAE2 knockdown (30) (Supplementary Figure S2B, right panel). Furthermore, a cumulative analysis of miR-34b/c target versus non-target transcripts shows SAE2 knockdown significantly suppressed gene expression of miR-34b/c target genes (Figure 3A, $P < 0.001$). To verify the mRNA-seq results, we used qRT-PCR and Western blot to examine gene expression and protein levels of six known miR-34 targets: c-Myc, c-Met, YY1, BCL-2, CDK4 and E2F3 (2–7). c-Myc is a major transcription factor, contributing to up to 70% of all human cancers (31). c-Met is a receptor tyrosine kinase that is involved in multiple signaling pathways and is a clinically validated cancer therapeutic target (32). YY1 is a transcription factor that has regulatory roles in cell proliferation, cell viability, epithelial–mesenchymal transition, metastasis, and drug/immune resistance (33). Bcl-2 is an anti-apoptotic protein and a clinically validated cancer therapeutic target (34). CDK4 is important for cell cycle G1-phase progression and a clinically validated cancer therapeutic target; its inhibitor received FDA 'breakthrough therapy' designation (35). E2F3 is a transcription factor that is suppressed by the retinoblastoma (Rb) protein; its activation due to mutations in the Rb gene is thought to be the driver for retinoblastoma and bladder cancer (36). Both mRNA and protein levels of the miR-34b/c targets were reduced by SAE2 knockdown in HCT116 (Figure 3B and C). In addition, these targets' mRNA were also reduced in LCL and RPMI-8226 cells upon SAE2 knockdown (Figure 3B), indicating the effect is cell-line independent. Similarly, in mouse xenograft HCT116 tumor tissues, IHC staining confirmed reduced levels of c-Myc and c-Met (Figure 3D). Because c-Myc, YY1 and E2F are transcription factors, GSEA analysis was performed that also indicated that their target gene sets were suppressed (Figure 3E and Supplementary Table S2). To rule out potential off-target effects of SAE2-targeting shRNA, we overexpressed WT shRNA-resistant SAE2-GFP in the presence of SAE2 knockdown. Expression of SAE2-GFP restored global SUMOylation when the endogenous SAE2 was knocked down (Supplementary Figure S3A), suppressed the increase of miR-34b/c expression due to knockdown of the endogenous SAE2 (Supplementary Figure S3B, left), and rescued expression of c-Myc and c-Met (Supplementary Figure S3B, right). These data suggest that the effect of SAE2 knockdown on miR-34b/c expression is due to on-target effects.

Next, we investigated whether the reduced level of miR-34b/c target expression due to SUMOylation inhibition is indeed dependent on miR-34b/c. Previous studies showed that although enforced expression of several miR-34 family members reduced c-Myc expression, miR-34c was the most potent in inhibiting c-Myc expression (37). Therefore, we evaluated the effects of anti-miR-34c. Anti-miR-34c rescued the effects of SAE2 knockdown on tested miR-34b/c targets (c-Myc, c-Met, E2F, Bcl-2, YY1, and CDK4) (Figure 4A), and restored c-Myc and c-Met protein levels (Figure 4B). Taken together, these data indicate that SUMOylation inhibition reduces c-Myc and c-Met expression, at least in part, through miR-34b/c induction.

SUMOylation regulates miR-34b/c expression and FOXO3a nuclear localization

Next, we investigated whether knockdown of SAE2 causes increased miR-34b/c through transcription of pri-miRNAs. Upon Ubc9 or SAE2 knockdown, pri-miR-34b/c expression level showed a significant increase relative to control; in contrast, upon ectopic expression of Ubc9 or SAE2, pri-miR-34b/c expression level showed a significant decrease, in both HCT116 and LCL cells (Figure 5A and Supplementary Figure S4). Consistent with this, knockdown of Ubc9 and SAE2 significantly increased mature miR-34b and c lev-

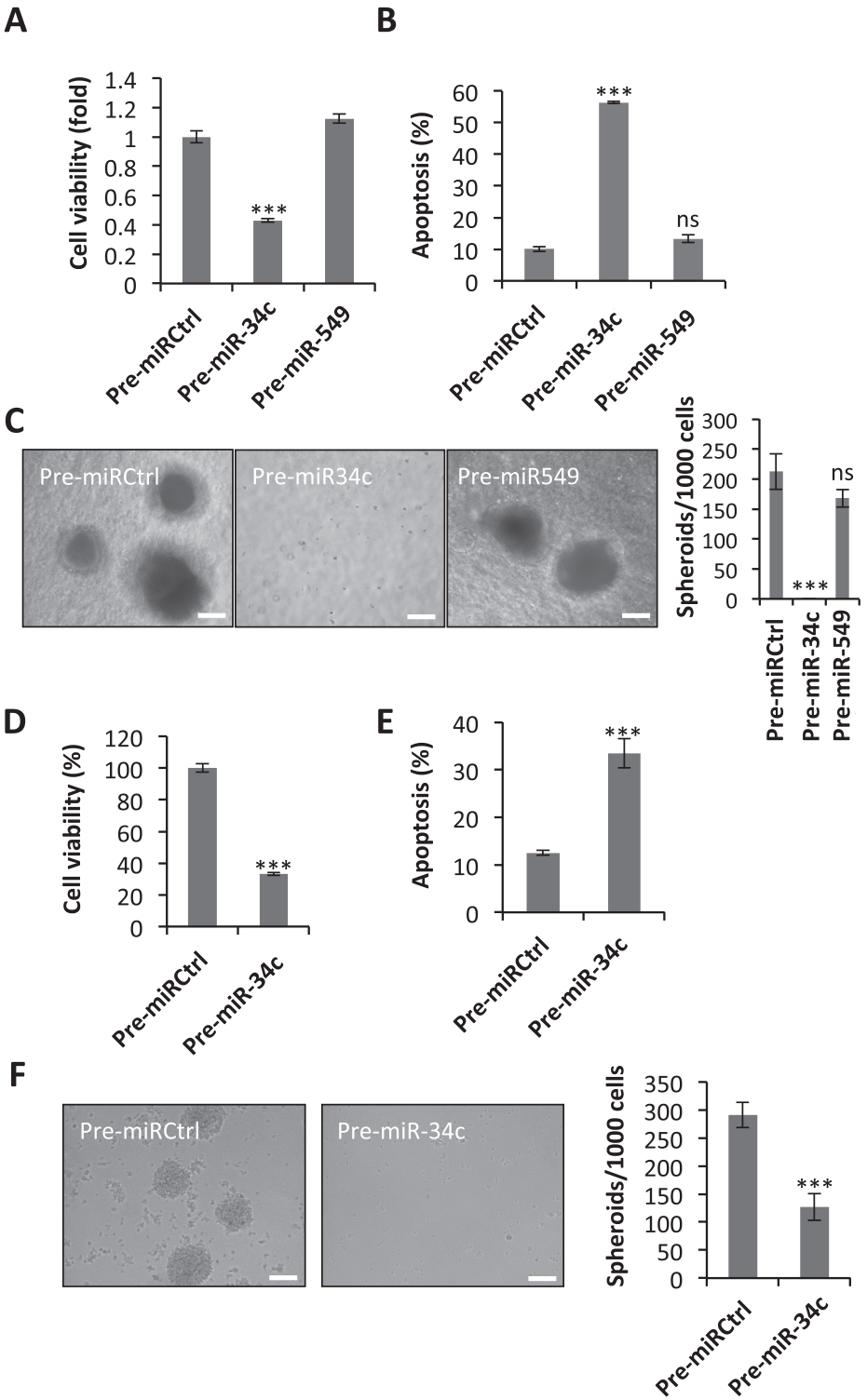

Figure 2. Elevated miR-34c is associated with anti-tumor effects. Individual pre-miRNA-34c and -549 were transfected into HCT116 or LCL cells. All pre-miRNAs were first transfected into cells for 2 days, followed by a second transfection to ensure transfection efficiency. (**A**, **D**) Cell viability was measured and normalized to control transfection (Pre-miRCtrl) in HCT116 (A) or LCL (D) cells. (**B**, **E**) Apoptosis was analyzed using Annexin V/PI staining after pre-miRNA transfection for 5 days in HCT116 (B) or LCL (E) cells. The results were then normalized to the control (pre-miRCtrl). (**C**, **F**) Soft agar transformation assay was conducted after pre-miRNA transfection in HCT116 (C) or LCL (F) cells. After 5 days of transfection, cells were counted and plated in 24-well soft agar plates and cultured for 21 days. Tumor spheroids were counted from four replicate wells and the results are presented in the bar graph. White bars in the images correspond to 100 μm. All results shown as means ± STDEV from three independent experiments. Statistical significance of the data was analyzed using one-way ANOVA and $P < 0.05$ was considered statistically significant. ***$P < 0.001$; ns, not significant, $P > 0.05$.

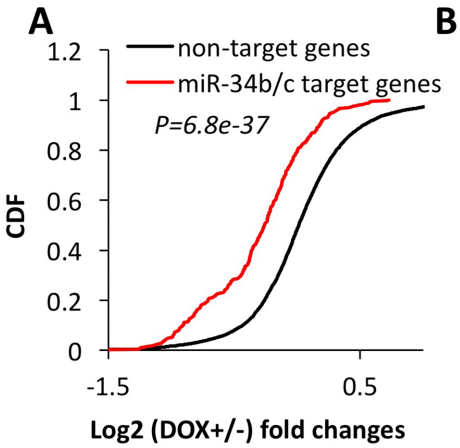

B

Cell line \ Gene name		MYC	MET	E2F3	YY1	CDK4	BCL2
HCT116	**Fold change**	**0.26**	**0.66**	**0.48**	**0.46**	**0.77**	**0.57**
	STDEV	0.08	0.01	0.02	0.05	0.07	0.10
	p vaule	***	***	**	***	**	**
LCL	**Fold change**	**0.60**	**0.48**	**0.45**	**0.70**	**0.64**	**0.79**
	STDEV	0.13	0.06	0.04	0.03	0.003	0.01
	p vaule	*	***	***	***	***	**
RPMI 8226	**Fold change**	**0.36**	**0.28**	**0.29**	**0.43**	**0.53**	**0.56**
	STDEV	0.04	0.02	0.05	0.01	0.01	0.04
	p vaule	***	***	***	***	***	***

*, P<0.05; **, P<0.01; ***, P<0.001

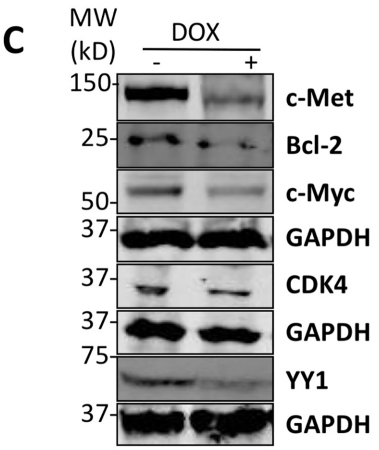

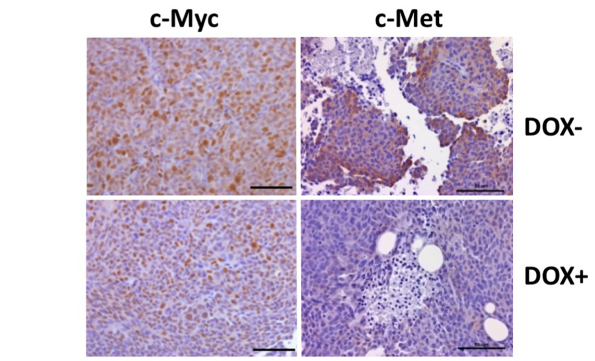

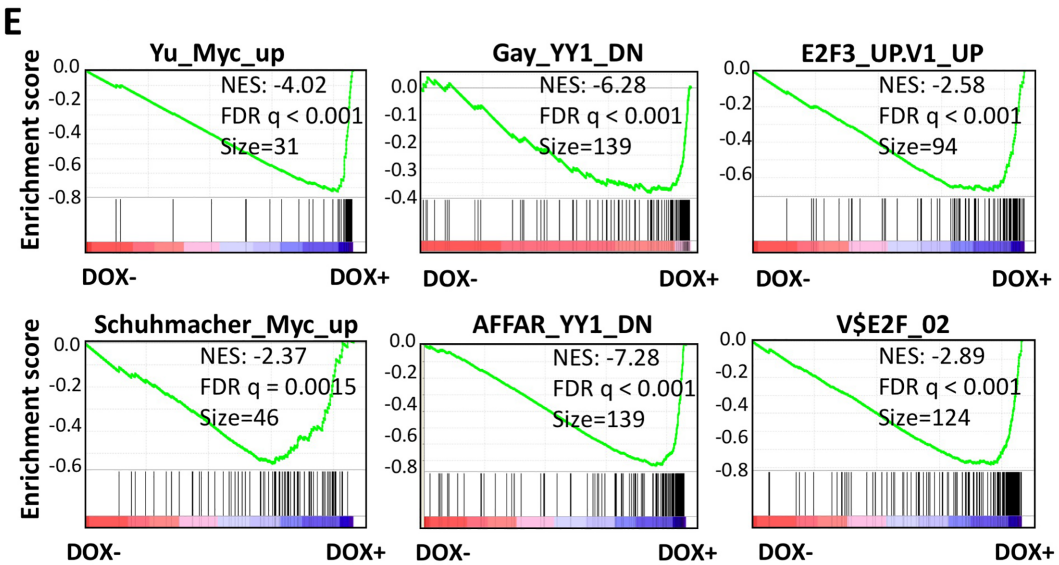

Figure 3. The expression of miR-34b/c-targeted genes was down-regulated upon SUMOylation inhibition. (**A**) Cumulative distribution plot (CDF) of log2-gene expression fold changes for miR-34b/c targeted genes (red) and all other expressed genes (black) after DOX-induced SAE2 knockdown in HCT116. mRNA-seq was performed following two individual DOX-induced shRNA-targeted SAE2 knockdowns in HCT116 cells for 5 days. Shown as the mean of the fold changes from two individual Ribo-zero RNA-seq results. (B, C) Verification of miR-34b/c target gene expression by qRT-PCR in the indicated cell lines (**B**), and in Western blot of HCT116 cells (**C**) after SAE2 knockdown. *MYC*, *MET*, *YY1, BCL2, CDK4* and *E2F3* mRNA levels were first normalized against GAPDH and then compared with the control (DOX-) in (B). GAPDH was used as the loading control in (C). All results shown are from three individual SAE2 knockdown experiments. Statistical significance of the data were analyzed using STDEV and one-way ANOVA. $^{*}P < 0.05$; $^{**}P < 0.01$; $^{***}P < 0.001$. (**D**) c-Myc and c-Met expression in xenograft tumor tissues with DOX-induced SAE2 knockdown examined by IHC staining. Black bar represents 50 μm. (**E**) GSEA shows the downstream targets of miR-34b/c targeted transcription factors in response to SAE2 knockdown.

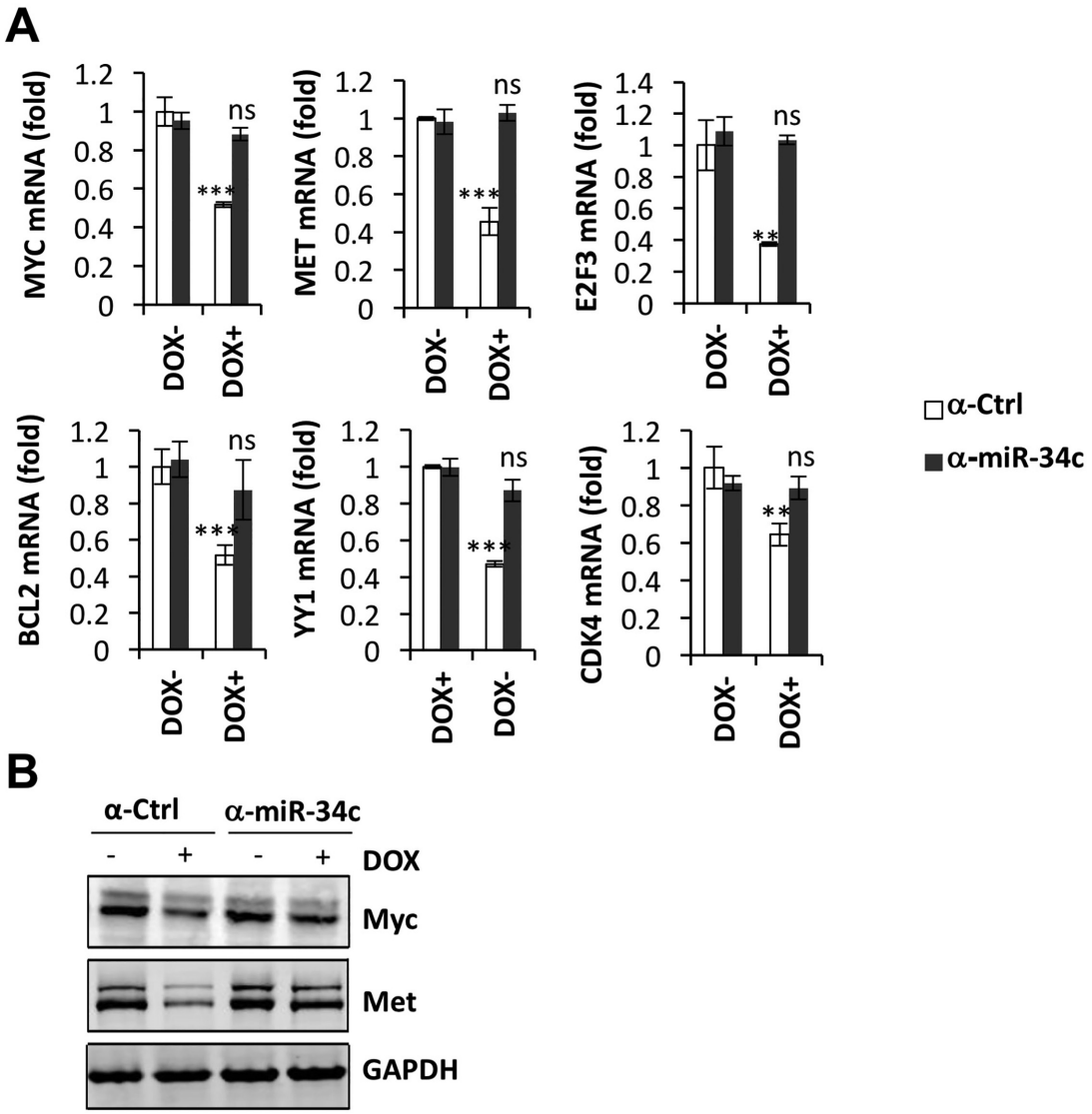

Figure 4. Anti-miR experiments link SUMOylation to miR-34b/c targets. (**A**) Anti-miR-34c (α-miR-34c) or anti-miR-Ctrl (α-Ctrl) were transfected into an HCT116 DOX-inducible SAE2 knockdown cell line. While DOX was added to induce SAE2 knockdown (DOX+), anti-miRs were transfected to the cells at the same time. Then miR-34c target genes, *MYC, MET, E2F3, BCL2, YY1,* and *CDK4* mRNA levels were detected using qRT-PCR and subsequently normalized, either with *GAPDH* mRNA (for mRNA) or *RNU6B* snRNA (for miRNA). (**B**) c-Myc and c-Met protein levels from the above experiments were also examined by western blot. All results shown as mean ± STDEV from three independent experiments. Statistical significance of the data were analyzed using one-way ANOVA. $^{*}P < 0.05$; $^{**}P < 0.01$; $^{***}P < 0.001$.

els, whereas ectopic expression of Ubc9 and SAE2 significantly reduced mature miR-34b and c level in both HCT116 and LCL cells (Figure 5B and Supplementary Figure S4). Knockdown or overexpression of SAE2 and Ubc9 had similar effects on pri-miR-34b/c expression. Therefore, these results indicate that SUMOylation regulates miR-34b/c gene expression.

In searching for transcription factors that potentially act on miR-34b/c expression, we used the UCSC Genome Browser (genome.ucsc.edu) ChIP-seq data of nearly 400 DNA-binding proteins to identify proteins that bind at the miR-34b/c promoter. The proteins that were found to bind or predicted to bind to the miR-34b/c promoter are CTCF, Myb, Sp1, FOXO3a, E2F, AP1 and p53. We evaluated the binding of these proteins to the miR-34b/c promoter using ChIP in the presence and absence of SAE2 knockdown. Among them, FOXO3a showed the largest changes (Figure 5C). In addition, we found that SAE2 knockdown increased FOXO3a accumulation in the nucleus, as shown by cell fractionation followed by western blot (Figure 5D) and IF (Figure 5E).

We also investigated whether FOXO3a is a SUMOylation substrate. We transfected FOXO3a into both His_6-SUMO1- and His_6-SUMO2-overexpressing HeLa cells (23), and purified FOXO3a under denaturing conditions to maximize preservation of SUMOylation. SUMO-modified FOXO3a was not detected in these cells (Supplementary Figure S5), indicating that it is not a SUMOylation substrate.

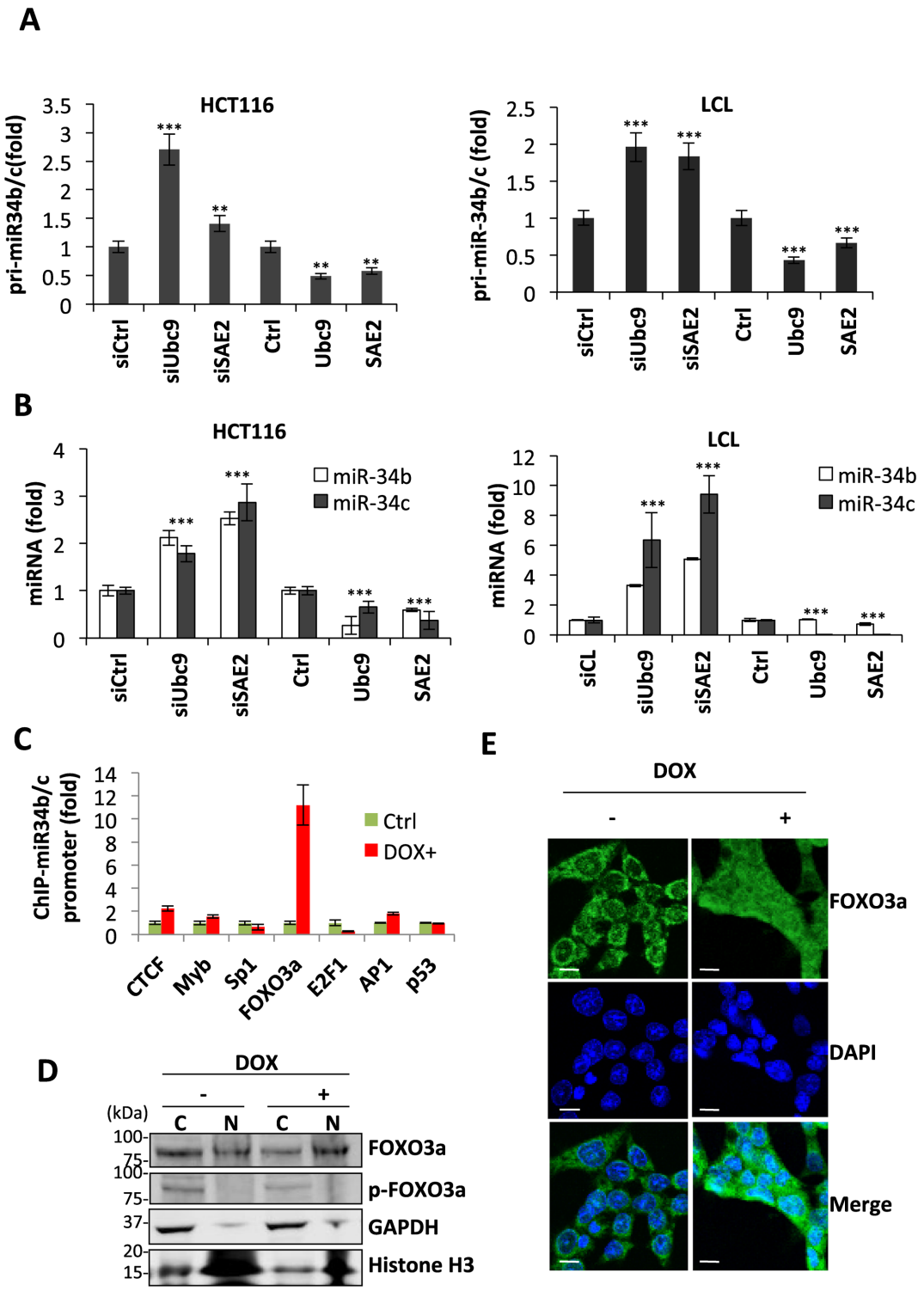

Figure 5. miR-34b/c expression is SUMOylation-dependent. (A, B) Pri-miR-34b/c (**A**) and mature miR-34b/c (**B**) were measured using qRT-PCR after either siRNA knockdown or ectopic expression of Ubc9 or SAE2 in HCT116 and LCL cells. Expression of pri-miR-34b/c was first normalized against GAPDH and then to the control (siCtrl). Expression of mature miR-34b/c was first normalized against RNU6B and then to the control. (**C**) Chromatin immunoprecipitation assay (ChIP) of transcription factors known or predicted to bind the miR-34b/c promoter without (DOX–) or with (DOX+) SAE2 knockdown. The results were normalized to total DNA input. IgG was used as a control. (**D**) Nuclear localization of FOXO3a increased after SAE2 knockdown (DOX+). Cell fractionation was carried out to separate cytoplasm (C) and nuclei (N) fractions and then Western blot was used to detect FOXO3a, phosphorylated FOXO3a (p-FOXO3a, Ser253), GAPDH, and histone H3. (**E**) FOXO3a localization was also visualized using IF. DAPI staining shows nuclei. The white bar represents 10 μm. All results shown as mean ± STDEV from three independent experiments. Statistical significance of the data was analyzed using one-way ANOVA. $^{**}P < 0.01$; $^{***}P < 0.001$.

Regulation of miR-34b/c expression through Akt phosphorylation of FOXO3a

FOXO3a nuclear localization is regulated by phosphorylation by Akt (38). Using GSEA, we showed that the Akt pathway is suppressed by knockdown of SAE2 (Figure 6A). Previous studies have shown that Akt is SUMOylated at Lys276, and Akt SUMOylation increases Akt kinase activity (39–41). The Akt pathway is frequently activated in cancers, but its effect on the expression of the tumor suppressive miR-34 family has not been reported. Thus, we investigated whether the Akt pathway could play a role in the expression of the tumor-suppressor miR-34. First, we showed that SAE2 knockdown reduced SUMOylation of Akt in HCT-116 cells (Supplementary Figure S6). When we mutated the previously identified SUMOylation sites (Akt-K276R/E278A mutant) (39,40) and repeated the experiment, some Akt SUMOylation remained, suggesting that there may be other SUMOylation sites in Akt (Supplementary Figure S6). In addition, SAE2 knockdown significantly reduced Akt auto-phosphorylation and phosphorylation of a known Akt target, GSK3β (Figure 6B) (42). Akt protein level remained the same after SAE2 knockdown, suggesting that SUMOylation does not affect Akt stability (Figure 6B), consistent with previous findings (40,42). To investigate the role of Akt SUMOylation in miR-34b/c expression, we expressed Akt-WT or SUMOylation defective mutant Akt-K276R/E278A and examined miR-34c expression. Akt-K276R/E278A induced higher expression of miR-34c than ATK-WT (Figure 6C). In addition, knockdown of SAE2 enhanced miR-34c levels in control cells and cells expressing WT-Akt, but not in cells expressing mutant Akt-K276R/E278A (Figure 6C). This data indicates that Akt SUMOylation is involved in miR-34b/c expression. Consistent with this, Akt phosphorylation of FOXO3a at Ser253, which prevents FOXO3a nuclear localization (38), was reduced by SAE2 knockdown (Figure 6D).

To further establish the link between Akt phosphorylation of FOXO3a and miR-34b/c expression, we generated constructs that express WT FOXO3a, a phosphorylation-defective mutant FOXO3a (T32A/S253A/S315A; TM), or a phosphorylation mimic-mutant FOXO3a (T32D/S253D/S315D; TD), based on previously identified phosphorylation sites (38). Previous studies showed that TD-FOXO3a is impaired in nuclear localization, but TM-FOXO3a is not (43). We expressed WT-, TM- and TD-FOXO3a with or without SAE2 knockdown in HCT116 cells. The protein expression levels of WT-, TM-, and TD-FOXO3a were similar, and SAE2 knockdown was achieved (Supplementary Figure S7). Upon SAE2 knockdown, pri-miR-34b/c expression did not change in the presence of TD-FOXO3a; increased slightly in the presence of TM-FOXO3a, possibly due to endogenous FOXO3a; and increased significantly in the presence of WT-FOXO3a (Figure 6E). Taken together, these data indicate that FOXO3a phosphorylation at Akt phosphorylation sites suppresses miR-34b/c expression.

We conducted additional studies to further establish the link between Akt SUMOylation, FOXO3a, and miR-34b/c expression. We co-expressed WT-, TM- and TD-FOXO3a with either Akt-WT or mutant Akt-K276R/E278A and examined miR-34b/c expression (Figures S6B and S7C). Co-expression of WT-FOXO3a with Akt-K276R/E278A resulted in higher miR-34b/c expression than co-expression with Akt-WT (Figure 6F), suggesting that removing Akt SUMOylation enhanced miR-34b/c expression, as did knockdown of SAE2. In contrast, TM-FOXO3a enhanced miR-34c expression similarly when co-expressed with either Akt-WT or Akt-K276R/E278A, suggesting that miR-34c expression induced by the phosphorylation-defective FOXO3a was not affected by Akt activity. Taken together, our data indicate that Akt regulates miR-34b/c expression through FOXO3a.

DISCUSSION

The miRNA-34 family suppresses the expression of c-Myc and other proteins functioning in the cell cycle, differentiation, and apoptosis pathways. In concert with this, miR-34 is down-regulated in a wide range of tumor types (8–12). In this study, we found that increased expression of SAE2 or Ubc9 suppressed miR-34b/c expression, and that knockdown of SAE2 or Ubc9 increased the expression of miR-34b/c. In addition, we identified Akt-mediated FOXO3a phosphorylation as a mechanism through which SUMOylation confers such function. Therefore, our study reveals a new function of Akt: regulating miR-34b/c expression. miR-34a expression is not affected by SAE2 knockdown (Supplementary Figure S2), suggesting that the effect of Akt-mediated FOXO3a phosphorylation and SUMOylation is specific to miR-34b/c expression (Figure 6). Our finding is consistent with previous reports that FOXO3a does not regulate miR-34a expression (44).

Previous studies suggested that miR-34b/c expression is regulated by p53 (44,45), which is also a SUMOylation substrate. However, we found that SAE2 or Ubc9 siRNA knockdown in isogenic WT ($p53^{+/+}$) and p53 deletion mutant ($p53^{-/-}$) HCT116 cell lines similarly increased pri-miR-34b/c expression (Supplementary Figure S8), suggesting that p53 is not involved in SUMOylation-dependent regulation of miR-34b/c. These findings are consistent with previous report that induction of miR-34b/c expression can occur in p53-null cells (37,44). Consistent with this, SAE2 knockdown increased FOXO3a but not p53 binding to the miR-34b/c promoter site, as shown by ChIP experiments (Figure 5C).

A genome-wide RNAi screen conducted to identify synthetic lethal interactions with the KRas and c-Myc oncogenes identified a SUMO activating enzyme and conjugation enzyme as important for the function of these oncogenes (27,46). It was found that SUMOylation of c-Myc targets it to the proteasome for degradation (47); thus, one would expect inhibition of SUMOylation to stabilize c-Myc in cells. In contrast, we found that inhibition of SUMOylation reduced c-Myc mRNA and protein levels. Therefore, our finding indicates that the miR-34b/c-dependent mechanism contributes to the reduced c-Myc level. To further support this conclusion, we showed correlation of MYC and CDK4 gene expression with UBC9, the only E2 enzyme catalyzing SUMOylation, in more than 2,000 samples of tumor and normal tissues from various organs (Figure 7A) (48). The expression of other miR-34b/c targets also

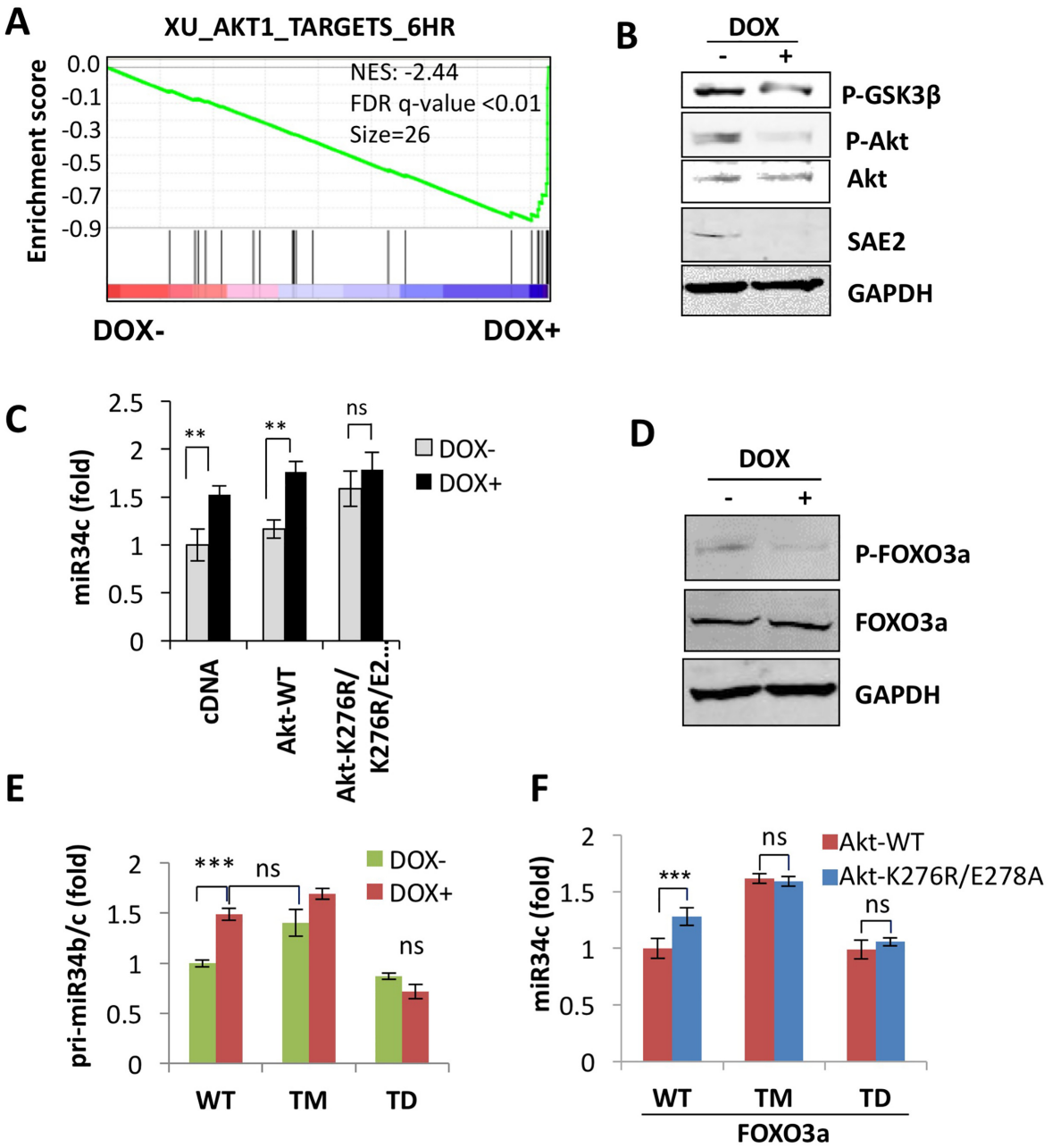

Figure 6. Akt regulates miR-34b/c expression through FOXO3a. (**A**) GSEA from genome-wide mRNA-seq shows Akt targets were down-regulated after SAE2 knockdown. (**B**) Knockdown of SAE2 reduced Akt auto-phosphorylation and its target GSK3β phosphorylation. GAPDH was used as a loading control. (**C**) Akt-WT and Akt-K276R/E278A were transfected into HCT116 cells with (DOX+) or without (DOX–) treatment one day earlier. After 2 days of DNA transfection and continued DOX treatment (DOX+), miR-34c levels were quantified using qRT-PCR. The results were first normalized against RNU6B and then to the empty vector transfection control. (**D**) After DOX-induced SAE2 knockdown, endogenous FOXO3a and phosphorylated FOXO3a (Ser253) (p-FOXO3a) were detected using Western blot. GAPDH was used as a loading control. (**E**) WT-, TM- or TD-FOXO3a was transfected into HCT116 cells treated with or without DOX-induced SAE2 knockdown for one day. Three days after DNA transfection (4 days after SAE2 knockdown), pri-miR-34b/c mRNA level was measured by qRT-PCR and the results were normalized to GAPDH mRNA, then knockdown was compared to control cells transfected with WT-FOXO3a. (**F**) Wild-type (Akt-WT) or SUMOylation-deficient mutant (Akt-K276R/E278A) Akt were co-transfected with WT-, TM- or TD-FOXO3a into HCT116 cells. After 2 days of DNA transfection, the cells were harvested and the miR-34c levels were quantified using qRT-PCR. The results were first normalized to RNU6B and then compared to Akt-WT and WT-FOXO3a co-expression. All results shown as mean ± STDEV from three independent experiments. Statistical significance of the data was analyzed using one-way ANOVA. $^{*}P < 0.05$; $^{***}P < 0.001$.

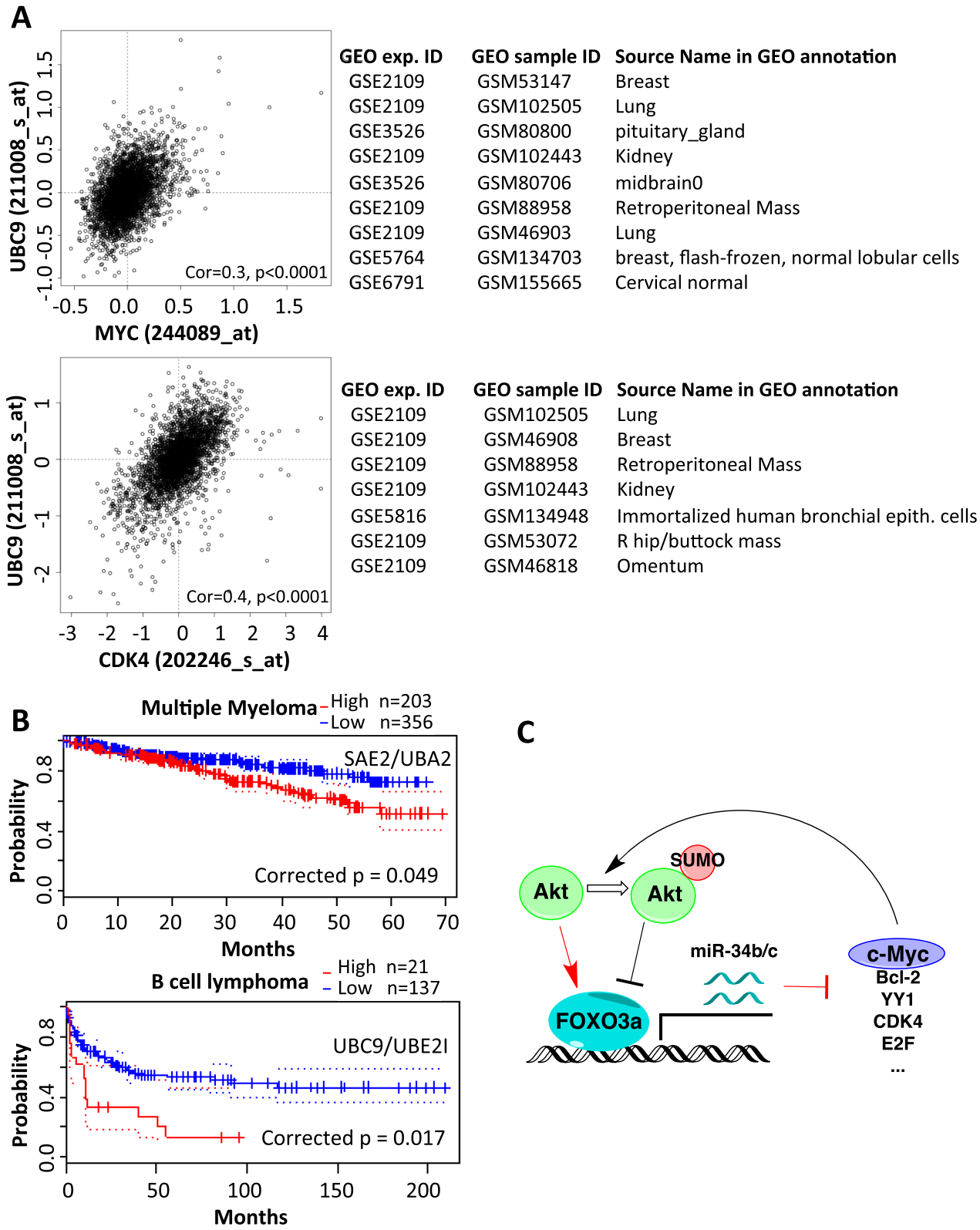

Figure 7. Importance of SUMOylation in miR-34-dependent oncogenesis pathways. (**A**) Correlation of Ubc9 (also known as UBE2I) expression to MYC (top) and CDK4 (bottom) as shown by the COXPRESdb program. The gene sets used are shown to the right of the correlation plots and contain more than 2,000 samples of tumor and normal tissues from various organs. (**B**) Kaplan–Meier analysis showing that elevated expression of SUMOylation enzymes (top panel, SAE2; bottom panel, Ubc9) correlates with poor prognosis in various cancers, as obtained from the Prognoscan database. (**C**) Our model shows how SUMOylation regulates the expression of genes important in driving oncogenesis, and how SUMOylation and c-Myc form a feed-forward loop that can be targeted to suppress oncogenesis. Inhibition of SUMOylation of Akt activates miR-34b/c expression that suppresses c-Myc levels, which further suppress the expression of SUMOylation machinery that leads to further inhibition of SUMOylation of Akt.

showed correlation with that of either SAE2 or UBC9 (Supplementary Figure S9). These findings support the link between SUMOylation and the miR-34-targeted gene expression program. Enzymes catalyzing SUMOylation are increased in various cancers, including colorectal, breast and ovarian cancers, lymphoma (49,50), and multiple myeloma (51–54). Furthermore, we showed that increased SUMOylation enzyme expression correlated with poor survival, using patient data from the Prognoscan database (55) (Figure 7B, multiple myeloma and Burkitt lymphoma). This finding is consistent with a previous report for colorectal cancer (25).

c-Myc was recently reported to act as a transcription factor for the SUMOylation machinery, including the SUMO proteins and the E1, E2 and E3 enzymes, in B-cell lymphoma (19). Along with this previous finding, our studies suggest the existence of a feed-forward loop in which inhibition of Akt SUMOylation leads to activation of miR-34b/c, which in turn reduces c-Myc production, leading to reduced SUMOylation enzyme that further enforces the suppression of Akt SUMOylation and the activation of miR-34 expression (Figure 7C).

In contrast to the prevailing view that SUMOylation has transcriptional suppressive functions (56), our finding provides an understanding of how SUMOylation can lead to enhancement of the expression of some proteins, such as c-Myc. This study also demonstrates how SUMOylation can regulate a target without directly modifying the target protein, and suggests a paradigm in which a post-translational modification alters the expression of miRNAs, which in turn target the expression of other cellular proteins.

DATA AVAILABILITY

All RNA-seq and miRNA-seq data have been deposited to the GEO database, which can be accessed by the link https://www.ncbi.nlm.nih.gov/geo/query/acc.cgi?acc=GSE101180.

SUPPLEMENTARY DATA

Supplementary Data are available at NAR Online.

ACKNOWLEDGEMENTS

We thank Drs Mark Boldin and Zuoming Sun for helpful discussions and comments and Dr Sarah T. Wilkinson for critical reading and editing of the manuscript. We thank the City of Hope Core Facilities for excellent technical support. The City of Hope Core Facilities are supported by the National Cancer Institute of the National Institutes of Health under award number P30CA033572. The content is solely the responsibility of the authors and does not necessarily represent the official views of the National Institutes of Health.

FUNDING

NIH [R01GM086171, R01CA212119, R01CA216987]; Tim Nesvig Lymphoma grant; Think *Cure*!, and Steven Gordon and Briskin Family Innovation Grant Program funding (to Y.C.). Funding for open access charge: NIH

Conflict of interest statement. Yuan Chen owns equity in SUMO Biosciences, Inc.

REFERENCES

1. Ha,M. and Kim,V.N. (2014) Regulation of microRNA biogenesis. *Nat. Rev.. Mol. Cell Biol.*, **15**, 509–524.
2. Kong,Y.W., Cannell,I.G., de Moor,C.H., Hill,K., Garside,P.G., Hamilton,T.L., Meijer,H.A., Dobbyn,H.C., Stoneley,M., Spriggs,K.A. *et al.* (2008) The mechanism of micro-RNA-mediated translation repression is determined by the promoter of the target gene. *Proc. Natl. Acad. Sci. U.S.A.*, **105**, 8866–8871.
3. Migliore,C., Petrelli,A., Ghiso,E., Corso,S., Capparuccia,L., Eramo,A., Comoglio,P.M. and Giordano,S. (2008) MicroRNAs impair MET-mediated invasive growth. *Cancer Res.*, **68**, 10128–10136.
4. Cole,K.A., Attiyeh,E.F., Mosse,Y.P., Laquaglia,M.J., Diskin,S.J., Brodeur,G.M. and Maris,J.M. (2008) A functional screen identifies miR-34a as a candidate neuroblastoma tumor suppressor gene. *Mol. Cancer Res.: MCR*, **6**, 735–742.
5. Bao,J., Li,D., Wang,L., Wu,J., Hu,Y., Wang,Z., Chen,Y., Cao,X., Jiang,C., Yan,W. *et al.* (2012) MicroRNA-449 and microRNA-34b/c function redundantly in murine testes by targeting E2F transcription factor-retinoblastoma protein (E2F-pRb) pathway. *J. Biol. Chem.*, **287**, 21686–21698.
6. Antonini,D., Russo,M.T., De Rosa,L., Gorrese,M., Del Vecchio,L. and Missero,C. (2010) Transcriptional repression of miR-34 family contributes to p63-mediated cell cycle progression in epidermal cells. *J. Invest. Dermatol.*, **130**, 1249–1257.
7. Wang,A.M., Huang,T.T., Hsu,K.W., Huang,K.H., Fang,W.L., Yang,M.H., Lo,S.S., Chi,C.W., Lin,J.J. and Yeh,T.S. (2014) Yin Yang 1 is a target of microRNA-34 family and contributes to gastric carcinogenesis. *Oncotarget*, **5**, 5002–5016.
8. Roy,S., Levi,E., Majumdar,A.P. and Sarkar,F.H. (2012) Expression of miR-34 is lost in colon cancer which can be re-expressed by a novel agent CDF. *J. Hematol. Oncol.*, **5**, 58.
9. Yang,S., Li,Y., Gao,J., Zhang,T., Li,S., Luo,A., Chen,H., Ding,F., Wang,X. and Liu,Z. (2013) MicroRNA-34 suppresses breast cancer invasion and metastasis by directly targeting Fra-1. *Oncogene*, **32**, 4294–4303.
10. Jin,K., Xiang,Y., Tang,J., Wu,G., Li,J., Xiao,H., Li,C., Chen,Y. and Zhao,J. (2014) miR-34 is associated with poor prognosis of patients with gallbladder cancer through regulating telomere length in tumor stem cells. *Tumour Biol.*, **35**, 1503–1510.
11. Chim,C.S., Wong,K.Y., Qi,Y., Loong,F., Lam,W.L., Wong,L.G., Jin,D.Y., Costello,J.F. and Liang,R. (2010) Epigenetic inactivation of the miR-34a in hematological malignancies. *Carcinogenesis*, **31**, 745–750.
12. Di Martino,M.T., Leone,E., Amodio,N., Foresta,U., Lionetti,M., Pitari,M.R., Cantafio,M.E., Gulla,A., Conforti,F., Morelli,E. *et al.* (2012) Synthetic miR-34a mimics as a novel therapeutic agent for multiple myeloma: in vitro and in vivo evidence. *Clin. Cancer Res.*, **18**, 6260–6270.
13. Misso,G., Di Martino,M.T., De Rosa,G., Farooqi,A.A., Lombardi,A., Campani,V., Zarone,M.R., Gulla,A., Tagliaferri,P., Tassone,P. *et al.* (2014) Mir-34: a new weapon against cancer? *Mol. Ther. Nucleic Acids*, **3**, e194.
14. Yeh,E.T. (2009) SUMOylation and De-SUMOylation: wrestling with life's processes. *J. Biol. Chem.*, **284**, 8223–8227.
15. Melchior,F. (2000) SUMO–nonclassical ubiquitin. *Annu. Rev. Cell Dev. Biol.*, **16**, 591–626.
16. Song,J., Durrin,L.K., Wilkinson,T.A., Krontiris,T.G. and Chen,Y. (2004) Identification of a SUMO-binding motif that recognizes SUMO-modified proteins. *Proc. Natl. Acad. Sci. U.S.A.*, **101**, 14373–14378.
17. Song,J., Zhang,Z., Hu,W. and Chen,Y. (2005) Small ubiquitin-like modifier (SUMO) recognition of a SUMO binding motif: a reversal of the bound orientation. *J. Biol. Chem.*, **280**, 40122–40129.
18. He,L., He,X., Lim,L.P., de Stanchina,E., Xuan,Z., Liang,Y., Xue,W., Zender,L., Magnus,J., Ridzon,D. *et al.* (2007) A microRNA component of the p53 tumour suppressor network. *Nature*, **447**, 1130–1134.

19. Hoellein,A., Fallahi,M., Schoeffmann,S., Steidle,S., Schaub,F.X., Rudelius,M., Laitinen,I., Nilsson,L., Goga,A., Peschel,C. *et al.* (2014) Myc-induced SUMOylation is a therapeutic vulnerability for B-cell lymphoma. *Blood*, **124**, 2081–2090.
20. Robinson,M.D. and Oshlack,A. (2010) A scaling normalization method for differential expression analysis of RNA-seq data. *Genome Biol.*, **11**, R25.
21. Subramanian,A., Tamayo,P., Mootha,V.K., Mukherjee,S., Ebert,B.L., Gillette,M.A., Paulovich,A., Pomeroy,S.L., Golub,T.R., Lander,E.S. *et al.* (2005) Gene set enrichment analysis: A knowledge-based approach for interpreting genome-wide expression profiles. *Proc. Natl. Acad. Sci. U.S.A.*, **102**, 15545–15550.
22. Betel,D., Koppal,A., Agius,P., Sander,C. and Leslie,C. (2010) Comprehensive modeling of microRNA targets predicts functional non-conserved and non-canonical sites. *Genome Biol.*, **11**, R90.
23. Tatham,M.H., Rodriguez,M.S., Xirodimas,D.P. and Hay,R.T. (2009) Detection of protein SUMOylation in vivo. *Nat. Protoc.*, **4**, 1363–1371.
24. Boggio,R., Colombo,R., Hay,R.T., Draetta,G.F. and Chiocca,S. (2004) A mechanism for inhibiting the SUMO pathway. *Mol. Cell*, **16**, 549–561.
25. Du,L., Li,Y.J., Fakih,M., Wiatrek,R.L., Duldulao,M., Chen,Z., Chu,P., Garcia-Aguilar,J. and Chen,Y. (2016) Role of SUMO activating enzyme in cancer stem cell maintenance and self-renewal. *Nat. Commun.*, **7**, 12326.
26. Yu,B., Swatkoski,S., Holly,A., Lee,L.C., Giroux,V., Lee,C.S., Hsu,D., Smith,J.L., Yuen,G., Yue,J. *et al.* (2015) Oncogenesis driven by the Ras/Raf pathway requires the SUMO E2 ligase Ubc9. *Proc. Natl. Acad. Sci. U.S.A.*, **112**, E1724–E1733.
27. Kessler,J.D., Kahle,K.T., Sun,T., Meerbrey,K.L., Schlabach,M.R., Schmitt,E.M., Skinner,S.O., Xu,Q., Li,M.Z., Hartman,Z.C. *et al.* (2012) A SUMOylation-dependent transcriptional subprogram is required for Myc-driven tumorigenesis. *Science*, **335**, 348–353.
28. Mo,Y.Y., Yu,Y., Theodosiou,E., Ee,P.L. and Beck,W.T. (2005) A role for Ubc9 in tumorigenesis. *Oncogene*, **24**, 2677–2683.
29. He,X., Riceberg,J., Pulukuri,S.M., Grossman,S., Shinde,V., Shah,P., Brownell,J.E., Dick,L., Newcomb,J. and Bence,N. (2015) Characterization of the loss of SUMO pathway function on cancer cells and tumor proliferation. *PLoS One*, **10**, e0123882.
30. Toyota,M., Suzuki,H., Sasaki,Y., Maruyama,R., Imai,K., Shinomura,Y. and Tokino,T. (2008) Epigenetic silencing of microRNA-34b/c and B-cell translocation gene 4 is associated with CpG island methylation in colorectal cancer. *Cancer Res.*, **68**, 4123–4132.
31. Dang,C.V. (2012) MYC on the path to cancer. *Cell*, **149**, 22–35.
32. Karagonlar,Z.F., Korhan,P. and Atabey,N. (2015) Targeting c-Met in cancer by MicroRNAs: potential therapeutic applications in hepatocellular carcinoma. *Drug Dev. Res.*, **76**, 357–367.
33. Shi,J., Hao,A., Zhang,Q. and Sui,G. (2015) The role of YY1 in oncogenesis and its potential as a drug target in cancer therapies. *Curr. Cancer Drug Targets*, **15**, 145–157.
34. Del Poeta,G., Postorino,M., Pupo,L., Del Principe,M.I., Dal Bo,M., Bittolo,T., Buccisano,F., Mariotti,B., Iannella,E., Maurillo,L. *et al.* (2016) Venetoclax: Bcl-2 inhibition for the treatment of chronic lymphocytic leukemia. *Drugs Today*, **52**, 249–260.
35. Owsley,J., Jimeno,A. and Diamond,J.R. (2016) Palbociclib:CDK4/6 inhibition in the treatment of ER-positive breast cancer. *Drugs Today*, **52**, 119–129.
36. Seville,L.L., Shah,N., Westwell,A.D. and Chan,W.C. (2005) Modulation of pRB/E2F functions in the regulation of cell cycle and in cancer. *Curr. Cancer Drug Targets*, **5**, 159–170.
37. Cannell,I.G., Kong,Y.W., Johnston,S.J., Chen,M.L., Collins,H.M., Dobbyn,H.C., Elia,A., Kress,T.R., Dickens,M., Clemens,M.J. *et al.* (2010) p38 MAPK/MK2-mediated induction of miR-34c following DNA damage prevents Myc-dependent DNA replication. *Proc. Natl. Acad. Sci. U.S.A.*, **107**, 5375–5380.
38. Brunet,A., Bonni,A., Zigmond,M.J., Lin,M.Z., Juo,P., Hu,L.S., Anderson,M.J., Arden,K.C., Blenis,J. and Greenberg,M.E. (1999) Akt promotes cell survival by phosphorylating and inhibiting a Forkhead transcription factor. *Cell*, **96**, 857–868.
39. Li,R., Wei,J., Jiang,C., Liu,D., Deng,L., Zhang,K. and Wang,P. (2013) Akt SUMOylation regulates cell proliferation and tumorigenesis. *Cancer Res.*, **73**, 5742–5753.
40. Lin,C.H., Liu,S.Y. and Lee,E.H. (2016) SUMO modification of Akt regulates global SUMOylation and substrate SUMOylation specificity through Akt phosphorylation of Ubc9 and SUMO1. *Oncogene*, **35**, 595–607.
41. de la Cruz-Herrera,C.F., Campagna,M., Lang,V., del Carmen Gonzalez-Santamaria,J., Marcos-Villar,L., Rodriguez,M.S., Vidal,A., Collado,M. and Rivas,C. (2015) SUMOylation regulates AKT1 activity. *Oncogene*, **34**, 1442–1450.
42. Li,R., Wei,J., Jiang,C., Liu,D.M., Deng,L., Zhang,K. and Wang,P. (2013) Akt SUMOylation regulates cell proliferation and tumorigenesis. *Cancer Res.*, **73**, 5742–5753.
43. Nakae,J., Barr,V. and Accili,D. (2000) Differential regulation of gene expression by insulin and IGF-1 receptors correlates with phosphorylation of a single amino acid residue in the forkhead transcription factor FKHR. *EMBO J.*, **19**, 989–996.
44. Kress,T.R., Cannell,I.G., Brenkman,A.B., Samans,B., Gaestel,M., Roepman,P., Burgering,B.M., Bushell,M., Rosenwald,A. and Eilers,M. (2011) The MK5/PRAK kinase and Myc form a negative feedback loop that is disrupted during colorectal tumorigenesis. *Mol. Cell*, **41**, 445–457.
45. Corney,D.C., Flesken-Nikitin,A., Godwin,A.K., Wang,W. and Nikitin,A.Y. (2007) MicroRNA-34b and MicroRNA-34c are targets of p53 and cooperate in control of cell proliferation and adhesion-independent growth. *Cancer Res.*, **67**, 8433–8438.
46. Luo,J., Emanuele,M.J., Li,D., Creighton,C.J., Schlabach,M.R., Westbrook,T.F., Wong,K.K. and Elledge,S.J. (2009) A genome-wide RNAi screen identifies multiple synthetic lethal interactions with the Ras oncogene. *Cell*, **137**, 835–848.
47. Gonzalez-Prieto,R., Cuijpers,S.A., Kumar,R., Hendriks,I.A. and Vertegaal,A.C. (2015) c-Myc is targeted to the proteasome for degradation in a SUMOylation-dependent manner, regulated by PIAS1, SENP7 and RNF4. *Cell Cycle*, **14**, 1859–1872.
48. Okamura,Y., Aoki,Y., Obayashi,T., Tadaka,S., Ito,S., Narise,T. and Kinoshita,K. (2015) COXPRESdb in 2015: coexpression database for animal species by DNA-microarray and RNAseq-based expression data with multiple quality assessment systems. *Nucleic Acids Res.*, **43**, D82–D86.
49. Hummel,M., Bentink,S., Berger,H., Klapper,W., Wessendorf,S., Barth,T.F., Bernd,H.W., Cogliatti,S.B., Dierlamm,J., Feller,A.C. *et al.* (2006) A biologic definition of Burkitt's lymphoma from transcriptional and genomic profiling. *N. Engl. J. Med.*, **354**, 2419–2430.
50. Richter,J., Schlesner,M., Hoffmann,S., Kreuz,M., Leich,E., Burkhardt,B., Rosolowski,M., Ammerpohl,O., Wagener,R., Bernhart,S.H. *et al.* (2012) Recurrent mutation of the ID3 gene in Burkitt lymphoma identified by integrated genome, exome and transcriptome sequencing. *Nat. Genet.*, **44**, 1316–1320.
51. Hanamura,I., Huang,Y., Zhan,F., Barlogie,B. and Shaughnessy,J. (2006) Prognostic value of cyclin D2 mRNA expression in newly diagnosed multiple myeloma treated with high-dose chemotherapy and tandem autologous stem cell transplantations. *Leukemia*, **20**, 1288–1290.
52. Zhan,F., Huang,Y., Colla,S., Stewart,J.P., Hanamura,I., Gupta,S., Epstein,J., Yaccoby,S., Sawyer,J., Burington,B. *et al.* (2006) The molecular classification of multiple myeloma. *Blood*, **108**, 2020–2028.
53. Zhan,F., Barlogie,B., Arzoumanian,V., Huang,Y., Williams,D.R., Hollmig,K., Pineda-Roman,M., Tricot,G., van Rhee,F., Zangari,M. *et al.* (2007) Gene-expression signature of benign monoclonal gammopathy evident in multiple myeloma is linked to good prognosis. *Blood*, **109**, 1692–1700.
54. Chen,L., Wang,S., Zhou,Y., Wu,X., Entin,I., Epstein,J., Yaccoby,S., Xiong,W., Barlogie,B., Shaughnessy,J.D. Jr. *et al.* (2010) Identification of early growth response protein 1 (EGR-1) as a novel target for JUN-induced apoptosis in multiple myeloma. *Blood*, **115**, 61–70.
55. Mizuno,H., Kitada,K., Nakai,K. and Sarai,A. (2009) PrognoScan: a new database for meta-analysis of the prognostic value of genes. *BMC Med. Genomics*, **2**, 18.
56. Flotho,A. and Melchior,F. (2013) Sumoylation: a regulatory protein modification in health and disease. *Annu. Rev. Biochem.*, **82**, 357–385.